COSY Beam Time Request

For Lab. use	
Exp. No.:	Session No. **13**

Collaboration: **JEDI**

Spin tune response to vertical orbit correction

Jülich, 17.07.2021

Spokespersons for the beam time*: **Artem Saleev (Ferrara/Jülich)**
Vera Shmakova (Jülich)
Paolo Lenisa (Ferrara)
Frank Rathmann (Jülich)

Spokespersons for the collaboration: **Paolo Lenisa (Ferrara)**
Jörg Pretz (Aachen/Jülich)

Address:
Institut für Kernphysik
Forschungszentrum Jülich
52428 Jülich
Germany

Phone: **+49 2461 61 5884** Fax: **+49 2461 61 3930**

E-mail: **a.saleev@fz-juelich.de**
v.shmakova@fz-juelich.de
f.rathmann@fz-juelich.de

lenisa@fe.infn.it
pretz@physik.rwth-aachen.de

Total number of particles and type of beam (p, d, polarization)	Kinetic energy (MeV)	Intensity or internal reaction rate (particles per second) minimum needed	Intensity or internal reaction rate (particles per second) maximum useful
Polarized deuterons	**~970 MeV/c**	**stored ~10^9**	**stored ~10^{10}**
Experimental area	Safety aspects (if any)	Earliest date of Installation	Total beam time (No. of shifts)
JEPO detector, solenoid of 2 MeV electron cooler, RF solenoid, Siberian snake, orbit correction, sextupoles, e-cooling	**None**	**No further installation required**	**2 MD + 4 weeks**

*We request a support from the LSF program of the EU.

Spin tune response to vertical orbit correction

A. Saleev[1,2], P. Lenisa[2], F. Rathmann[1], V. Shmakova[1], J. Pretz[1,3] on behalf of the JEDI Collaboration

[1]*IKP, Forschungszentrum Jülich, 52424 Jülich, Germany*
[2]*University of Ferrara, 44100 Ferrara, Italy*
[3]*III. Physikalisches Institut B, RWTH Aachen University, 52056 Aachen, Germany*

July 17, 2021

Abstract

Searches of electric dipole moments (EDM) of charged particles in pure magnetic rings, such as COSY, or electrostatic and hybrid magnetic-electric storage rings, planned in the future, require new methods to disentangle the EDM signal from the large background produced by magnetic dipole moments. In these experiments, the sources of systematic background are in-plane magnetic fields. It is important to distinguish the origins of the in-plane magnetic fields, which could be produced intentionally by vertical orbit correction to keep the beam on a closed path, or unintentionally due to the alignment errors of the magnets. We propose to use the method of spin tune mapping to determine the relative importance of two origins. At the first stage, the model of COSY should be verified for the spin tune shifts when vertical three-steerer closed-orbit bumps are applied. At the second stage, the spin tune responce to vertical orbit correction in the arcs will testify its contribution to the systematic background.

1 Introduction

The electric dipole moment (EDM) signal constitutes a rotation of the spin in the electric field. In an all magnetic ring (COSY), it is the motional electric field $\propto [\vec{\beta} \times \vec{B}]$ along the radial x-axis around which the EDM precesses. As such, an EDM contributes also to a constant tilt of the stable spin axis

$$\vec{c} = \vec{e}_y + \xi_{\mathrm{edm}} \vec{e}_x \tag{1}$$

On the other hand, nonuniform in-plane magnetic fields tilt the invariant spin axis towards x and z,

$$\vec{c} = c_y \vec{e}_y + (\xi_{\mathrm{edm}} + c_x^{\mathrm{mdm}}) \vec{e}_x + c_z^{\mathrm{mdm}} \vec{e}_z. \tag{2}$$

While $c_y \simeq 1$, the projections $c_{x,z}$ depend on the specific location along the beam path s, chosen to define the one-turn spin transfer matrix (see also discussion in ref.[1]). In-plane magnetic fields have two origins: one is the radial focusing fields of the quadrupoles and vertical steerers to control the beam on a closed orbit. Another one is imperfection fields produced by the uncontrolled alignment errors of the magnets. The spin rotations in the in-plane fields are non-commuting with the spin rotations around the vertical field of the dipoles. This leads to complex dependance of $\vec{c}$ on s. However, unlike $c_{x,z}^{\mathrm{mdm}}$, the EDM contribution to $\vec{c}$ is *invariant* along the orbit. It gives possibility to disentangle the EDM and Magnetic Dipole Moment (MDM) effects if non-invariant part of $\vec{c}$ can be described.

1.1 First stage: spin tune mapping with vertical closed-orbit three-steerer bumps

In the JEDI experiment `E010`, performed in 2020, we demonstrated the possibility to separate the contribution to $\vec{c}$ produced by the local vertical orbit bump made by vertical steerers MSV18, MSV20 and MSV22. As a first stage of new experiment, we propose to repeat the same measurement with 12 configurations of the bumps made by different consecutive three vertical steerers in the arcs at COSY.

Such measurement with the bump MSV18-20-22 had following scheme. The beam storage cycles had three time periods, $\Delta T_{1,2,3}$. At two of them, ΔT_1 and ΔT_3, all of the magnet settings were kept constant during the measurements (see Fig. 1), which means that the beam orbit measured in both

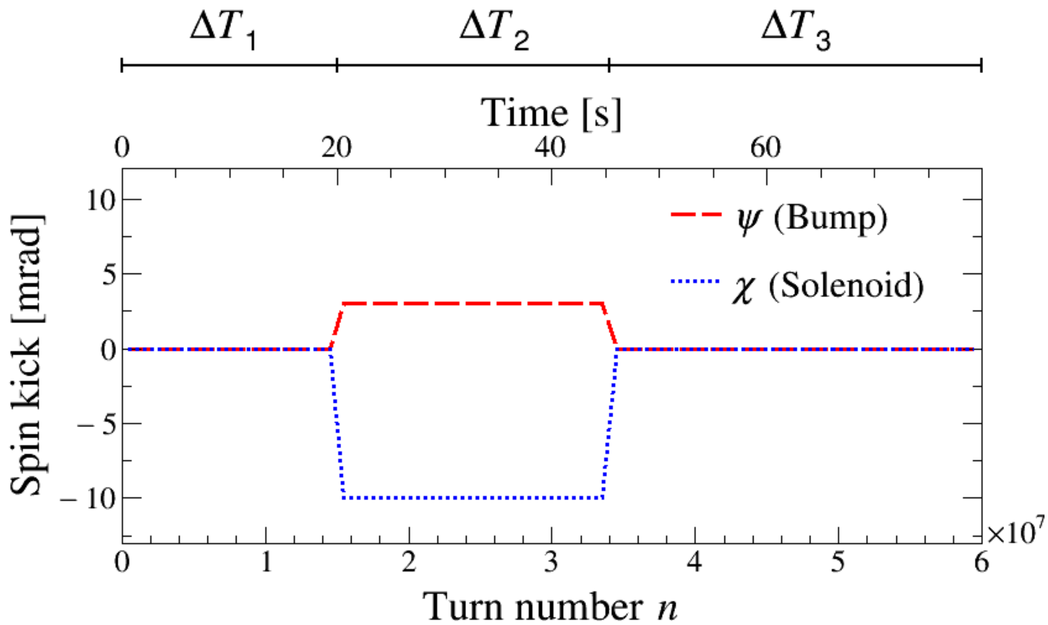

Figure 1: A scheme for switching on and off the bump and solenoids. The times ΔT_1, and ΔT_3 denote when the bump steerers and solenoids are switched off, and during the time ΔT_2 the bump steerers and solenoids are simultaneously switched on with constant currents.

intervals would be the same (see example of the orbit in ΔT_1 at Fig. 2). In a second period ΔT_2 the settings of three steerers (used to create a bump) and two solenoids have been varied after every two cycles. The solenoids were intended to work as spin rotators: a compensation solenoid of 2MeV e-cooler and a superconducting snake solenoid, both connected to bipolar power supplies. For every bump, steerer values ($\theta_{1,2,3}$) were set on top of the values which they had in intervals ΔT_1 and ΔT_3.

In order to set up strictly local bump, steerer values ($\theta_{1,2,3}$) should be chosen at a specific proportion to each other. As shown in ref.[2], the steerer settings can be calculated directly from the Orbit Responce Matrix, using two Beam Position Monitors m and n, located at $\pi/2$-betatron phase difference to each other (any BPMs outside of the bump region):

$$\begin{aligned} A_{m1}\theta_1 + A_{m2}\theta_2 + A_{m3}\theta_3 = 0 \\ A_{n1}\theta_1 + A_{n2}\theta_2 + A_{n3}\theta_3 = 0 \end{aligned} \tag{3}$$

where in case of measured ORM, θ_i is in units of %-setting of steerer

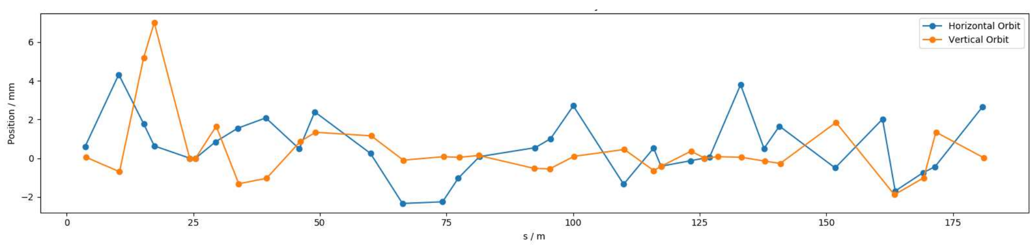

Figure 2: Example of the reference orbit measured in time interval ΔT_1 of the beam cycle.

power supply and A_{ji} is the ORM element for $i-$steerer and $j-$BPM (in [mm/%]). The setting of a central steerer in the bump, θ_2, can become a reference one to θ_1 and θ_3:

$$\theta_1 = \theta_2 \frac{A_{n3}A_{m2} - A_{n2}A_{m3}}{A_{n1}A_{m3} - A_{n3}A_{m1}} \tag{4}$$

$$\theta_3 = \theta_2 \frac{A_{m2}A_{n1} - A_{m1}A_{n2}}{A_{m1}A_{n3} - A_{m3}A_{n1}} \tag{5}$$

An advantage of this approach, is that θ_i becomes independent from the uncertainties of model parameters, such as the steerer's current-to-kick calibration factors. Those factors and other ucertainties are all inherently included in the measured ORM (see Fig.3), unlike in case of relation of θ_i through the beta-functions and beta-phases to create the bump. Eqs. $4, 5$ were used to calculate the settings for any bump made by 3 consecutive vertical steerers in the arcs, but in total only 4 different bumps were used during the beamtime. The example of coefficients K_1, K_3, that define relative settings $\theta_1 = K_1\theta_2$ of steerer MSV18 and $\theta_3 = K_3\theta_2$ of steerer MSV22 for bump MSV18-20-22 are shown on Fig. (4). Such coefficients were calculated for all of the vertical (phase-orthogonal) BPM pairs at COSY according to Eqs. $4, 5$ and put into the histograms. That allowed to discard K_1 and K_3 that come from potential errors of ORM measurement (which was partly automated and results were preliminary): the values with highest bin count were selected as a final ones. The same method for calculation of K_1 and K_3 in COSY-Infinity, while using the modelled ORM in units of mm/mrad, does not produce any distribution in the values $K_{1,3}$ (up to a machine precision), and therein allow to create strictly local bumps. In the orbit difference between ΔT_1 (shown on Fig. 2) and ΔT_2 when steerers were set on a proper values, one can see the vertical closed orbit bump. Measurements for two bumps, MSV 10-12-14 and MSV

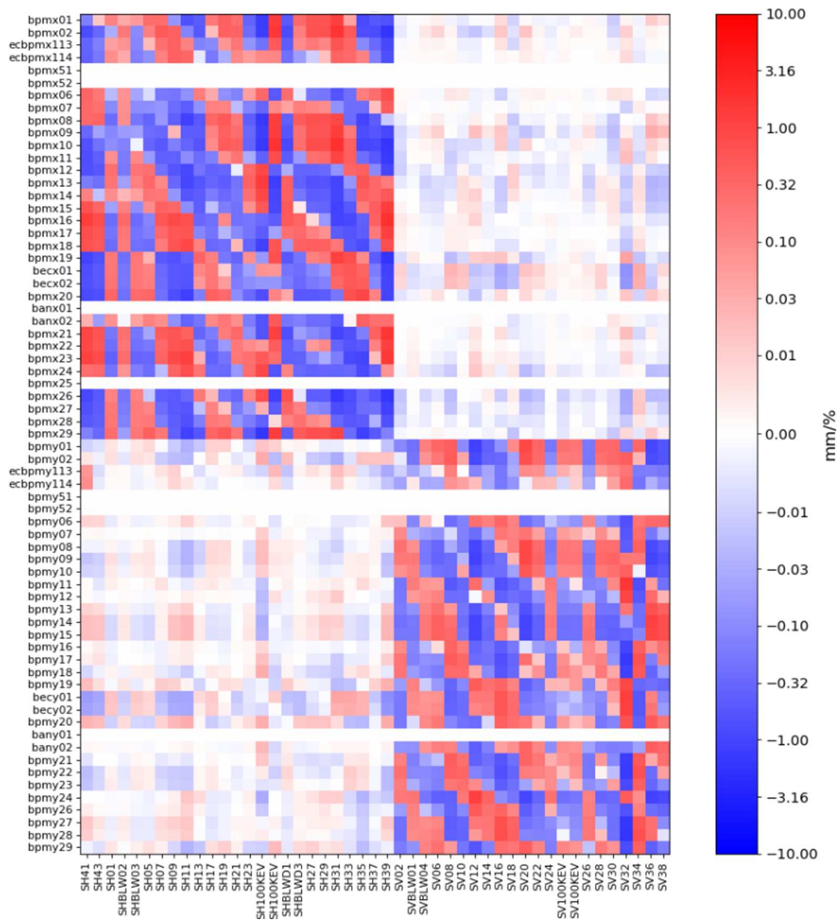

Figure 3: Orbit responce matrix that was measured during the machine development time preceding the experiment E010.

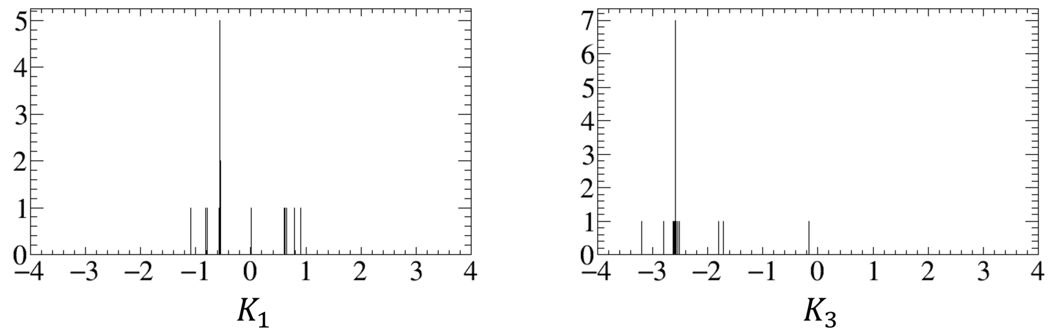

Figure 4: Analysis of the measured ORM to derive the ratio for steerers MSV18 (K_1) and MSV22 (K_3) to be used in the proportion to the setting of MSV20.

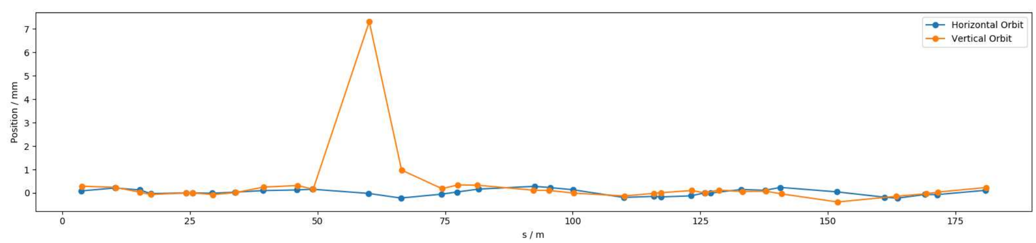

Figure 5: Example of the bump with steerers MSV 10 - 12 - 14. RMS orbit perturbation, excluding the BPMs within the bump, is: vertical 0.179 mm, horizontal 0.145 mm.

36-38-02 (Figs. 5, 6), were done only with unpolarized beam to explore the chromaticity dependence on the bump amplitude.

The bumps MSV 08-10-12 and MSV18-20-22 (Fig. 8) were used both with polarized and unpolarized beam. In the next section, the influence of those two bumps on the measured direction of the invariant spin axis $\vec{c}$ is discussed. It is worth to note that the reference orbit was different in those measurements (shown at Fig. 7). In total, the spin tune measurements were succesfull for 430 cycles with the bump MSV 18-20-22, and for 6 cycles with the bump MSV 08-10-12. Usage of property given by Eq. 4 allowed for the bumps to be sufficiently local, with RMS perturbation of the orbit except in the bump itself of less than 0.2mm. If the relative orbit shift in the ring would be larger, it would have an impact on the direction of $\vec{c}(s)$ and increase the systematic error for its definition.

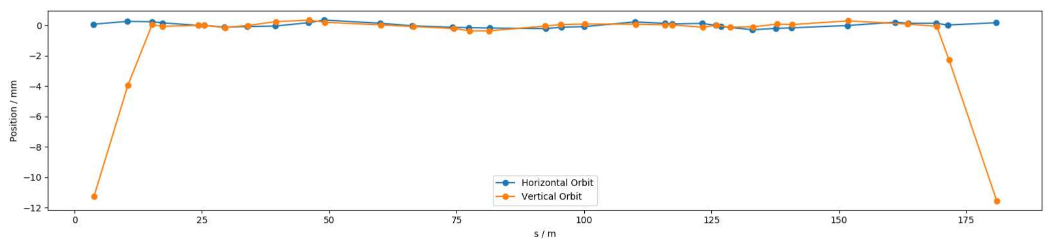

Figure 6: Example of the bump with steerers MSV 36 - 38 - 02. RMS orbit perturbation, excluding the BPMs within the bump, is: vertical 0.167 mm and horizontal 0.166 mm.

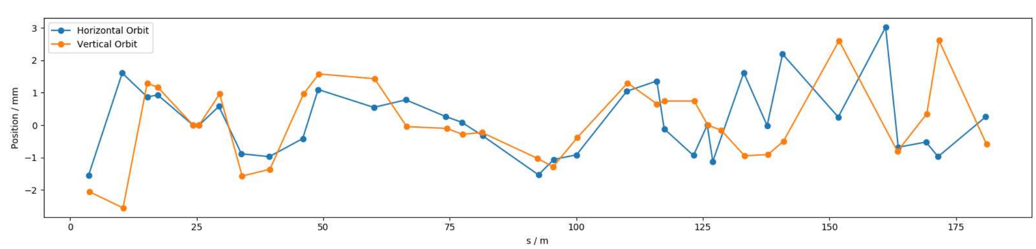

Figure 7: Example of another reference orbit measured in time interval ΔT_1 of the beam cycle.

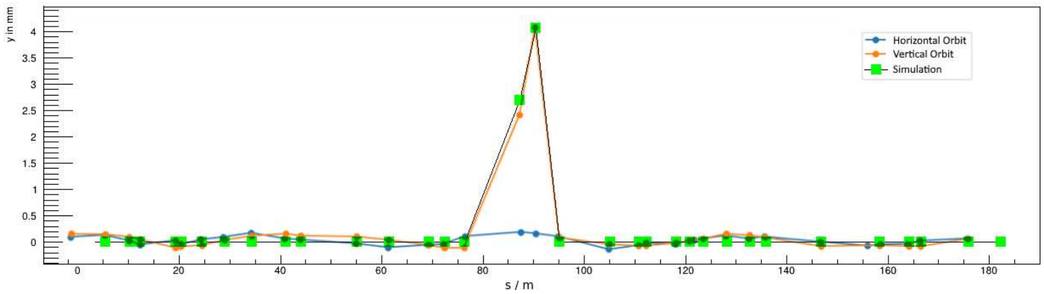

Figure 8: Example of the bump with steerers MSV 18-20-22, when SV20=-10%. Model prediction for vertical orbit is marked by green squares, and measured vertical orbit is orange circles (blue circles for horizontal orbit, while simulation for horizontal orbit is not shown as it is all zero).

1.2 Spin tune map with bump and one solenoid

The method of "spin tune mapping" with solenoids is based on the outstanding ability to determine the spin tune with a relative error of 1×10^{-10} during a 100 s long beam cycle at COSY from the time dependence of horizontal polarization [4]. It is thoroughly discussed in [5].

The spin rotation in the bump is predicted by spin tracking using COSY-Infinity [3]. It is similar to that caused by a weak helical snake, therefore it can be approximated by a point-like spin rotator at a certain azimuthal location in the ring. Effectively, it is a spin kick around a fixed in-plane axis at the place of solenoid, $\vec{w} = \vec{e}_x \sin\alpha + \vec{e}_z \cos\alpha$, where α is a directional angle that is counted from the positive axis z towards the positive axis x (see Fig. 9). Parameter α is specific for each bump. The magnitude of the spin kick ψ in the bump is proportional to the steerer kick angle θ (for example, of a central steerer as in Eqs. 4, 5) in the bump which is chosen as a reference one. The bump amplitude is also proportional to θ. Matching the measured difference orbit at the BPM with highest deviation to the model of the ideal bump (see Fig. 8), one could use the resulting values of the central steerer in the model (in mrad) and experiment (in %) as a reference for the current-to-kick calibration. Then, the values for other two steerers are obtained in the model by using Eqs. 4 and 5 for the modelled ORM. In the ideal COSY ring with ideal bump MSV 18-20-22, dependance of $\vec{c}$ on the location of observation point s, is shown in Fig. 12. Important locations are $s = 16.27$ m (here define $c_z = c_{\rm sol}$) for the 2 MeV e-cooler compensation

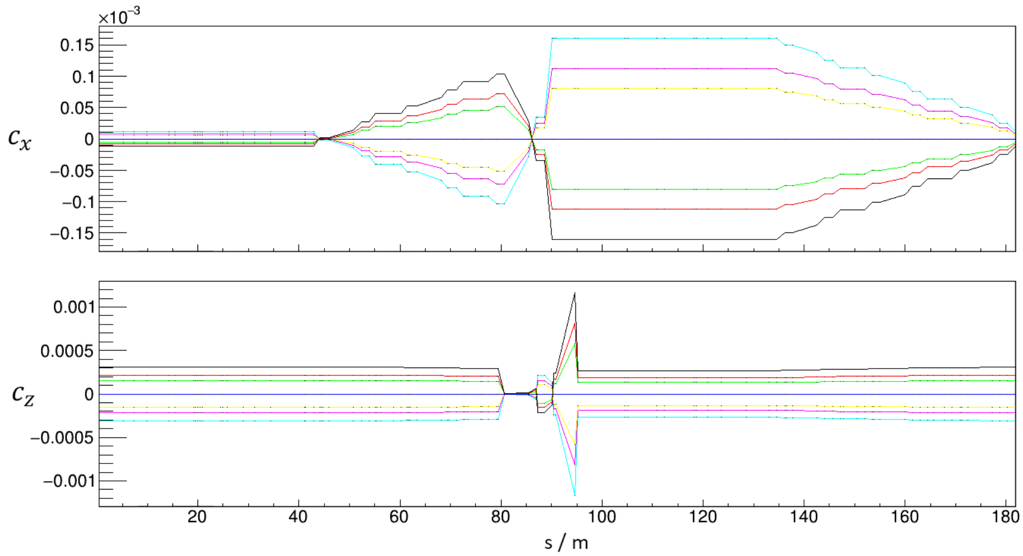

Figure 9: Dependence of the in-plane components of the invariant spin axis $\vec{c}$ along the closed orbit path s. Color code corresponds to the amplitudes of the bump SV 18-20-22 that were used during the measurement, from $-4\,\mathrm{mm}$ (cyan), $-3\,\mathrm{mm}$ (pink) to $2\,\mathrm{mm}$ (green), $3\,\mathrm{mm}$ (red), $4\,\mathrm{mm}$ (black). Amplitude $-2\,\mathrm{mm}$ (yellow) was not used for spin tune mapping.

solenoid in target telescope and at $s = 126.13\,\mathrm{m}$ (define $c_z = c_{\mathrm{snake}}$) for superconducting snake solenoid at cooler telescope.

The fits of steerer calibration kicks to the model of COSY in COSY-Infinity from the measured ORM, comparison of results with COSY-database values, are subjects of ongoing studies.

Only 2MeV e-cooler solenoid was used initially with the bump MSV 18-20-22. The bump steerers and the solenoid were switched on and off according to scheme on Fig.1, while the same settings repeated for 2 cycles. The spin tune shift $\Delta\nu_s$ that corresponds to the central flattop (ΔT_2) will have a

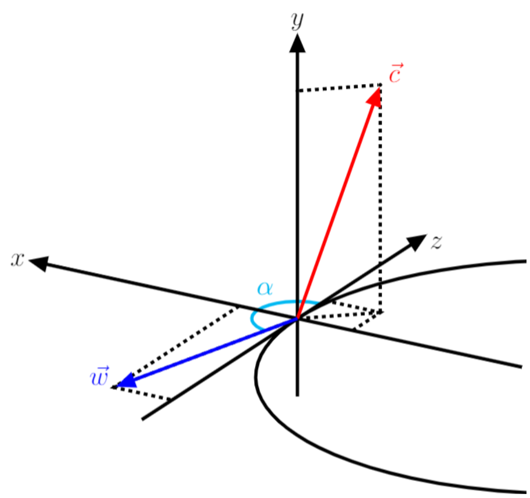

Figure 10: Relative orientation of vectors $\vec{c}$ and $\vec{w}$.

dependence on the crosstalk between solenoid and bump, given by:

$$\begin{aligned}\cos\pi(\nu_s+\Delta\nu_s) \quad = \quad & \cos\pi\nu_s\cos\frac{\psi}{2}\cos\frac{\chi}{2} \\ & -(\vec{c}^{\,\text{bump}}\cdot\vec{w})\sin\pi\nu_s\sin\frac{\psi}{2}\cos\frac{\chi}{2} \\ & -(\vec{c}^{\,\text{sol}}\cdot\vec{e}_z)\sin\pi\nu_s\cos\frac{\psi}{2}\sin\frac{\chi}{2} \\ & -\cos\alpha\sin\frac{\psi}{2}\sin\frac{\chi}{2}. \qquad (6)\end{aligned}$$

Unknown vectors $\vec{c}^{\,\text{sol}}$ and $\vec{c}^{\,\text{bump}}$ define the directions of the corresponding invariant spin axes at the locations of the solenoid and first steerer of the bump. Parameter $p1 = \cos\alpha\sin\frac{\psi}{2}$ can be determined independently from the other in-plane fields present in the ring. This means the solenoid acts as a benchmark for every bump,and $p1$ can be compared to the model prediction in which all other parameters are that of an ideal ring. The results of such comparison for MSV18-20-22 and 2MeV e-cooler solenoid are given in left top and bottom plots on Fig. 11.

1.3 Spin tune map with bump and two solenoids

When two static solenoids located at COSY telescopes are used, position dependence of $\vec{c}(s)$ is partly uncovered.

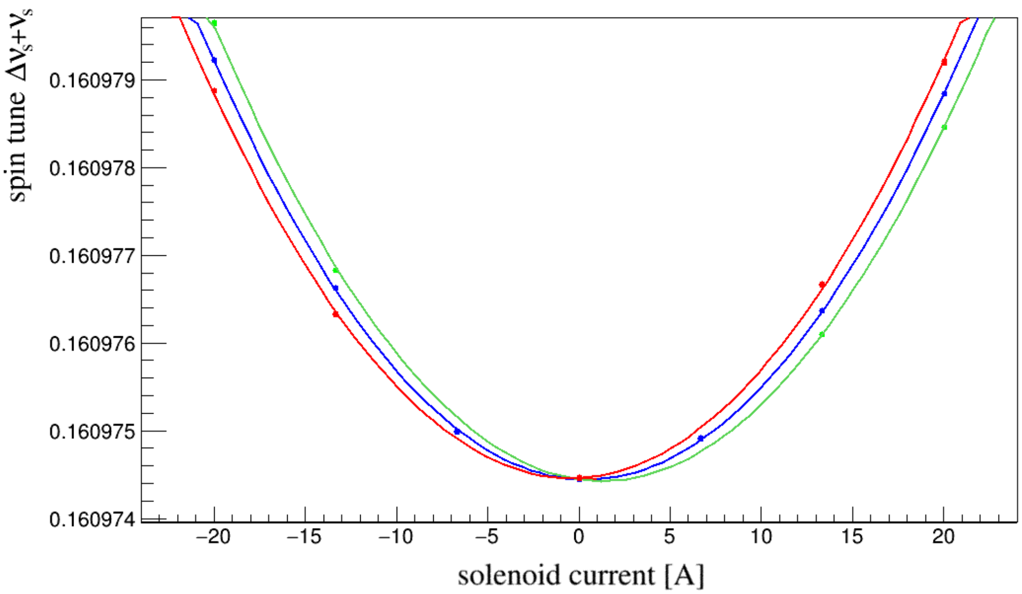

Figure 11: The spin tune measurements for two amplitudes of the bump MSV 18-20-22 marked as red points for $\theta = -10\%$, green points for $\theta = 11\%$. Blue points - no bump applied. All curves are parabolic fits. The minima for blue parabola indicates non-vanishing c_z according to third term in Eq. 6 . The shift of the minima for red and green curves is described by the last term in Eq. 6.

Among the spin tune measurement cycles for bump SV18-20-22, there are several sets with the same steerer settings that correspond to a specific bump amplitude. For each fixed bump amplitude, the spin tune shift with respect to the applied solenoid currents I_1, I_2 was determined. Such set of measurements on the grid of solenoid currents $I_{1,2}$ is called "spin tune map"[5]. Example of spin tune map for +3 mm amplitude of the bump SV18-20-22, is shown on Fig. 13. The spin tune shifts can be described by non-lattice model that suggests two solenoids as pure spin rotators. Eq. 6 transforms to:

$$-\pi\Delta\nu_s = (\cos a \cos b - 1)\cot \pi\nu_s - c_{\mathrm{sol}} \sin a \cos b - c_{\mathrm{snake}} \cos a \sin b - \frac{\sin a \sin b}{\sin \pi\nu_s}\,, \tag{7}$$

where

$$a = \frac{k_1\, I_1}{2} \quad \text{and} \quad b = \frac{k_2\, I_2}{2}\,. \tag{8}$$

and the solenoid's current-to-spin-kick calibration factors $k_{1,2}$ are free parameters. As a result of the spin tune mapping (see example on Fig. 13), the values of c_z are determined with angular precision $\sigma_{c_{\mathrm{sol}}} = 6.9\,\mu\mathrm{rad}$ at the 2 MeV e-cooler solenoid and $\sigma_{c_{\mathrm{snake}}} = 3.6\,\mu\mathrm{rad}$ at superconducting snake.

Fit results for spin tune maps at all of the measured bump amplitudes are in good agreement with the model prediction for dependence of c_z projections at solenoids from the central steerer setting (see slope parameter $p1$ in Fig. 11). Note that an offset parameter $p0$ at Fig. 11 is non-vanishing in case of measured c_{sol} and c_{snake} due to either the presence of alignment errors in the ring, or the effect of vertical closed orbit correction, or a complex mix of the two, which contribute to the tilt of invariant spin axis towards z-axis.

1.4 Systematic errors of the method

The spin tune shifts related to the spin tune drifts within the cycle and from cycle to cycle are also major indicators of the unwanted changes in the machine setup. The drift of the baseline spin tune ν_s (defined for reference orbit when bump steerers and solenoid are switched off in time intervals ΔT_1, ΔT_3) was as big as $\delta\nu_s \approx 2\times 10^{-7}$ over the span of two weeks. Spin tune drifts over 110 seconds of the beam cycle with RMS value for all cycles $3.7 \cdot 10^{-9}$ were considered as the main source of systematic errors for the spin tune shifts $\Delta\nu_s$, which is almost the same as in [5].

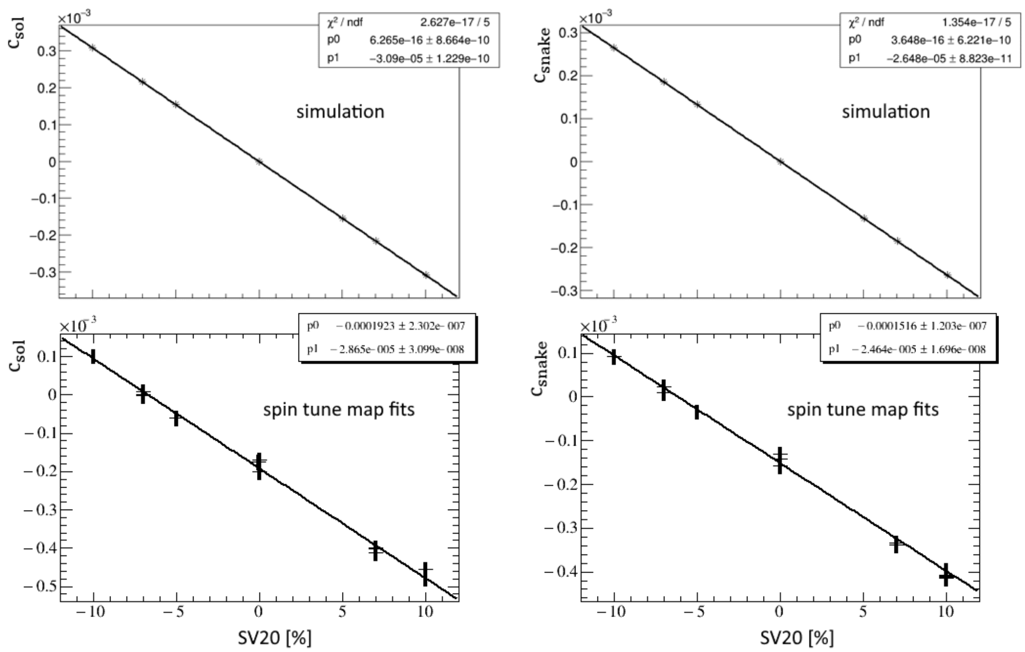

Figure 12: Dependence of the fit parameters $c_{\rm sol}$ and $c_{\rm snake}$ on the steerer setting and comparison to simulation results. Value +10% corresponds to the bump amplitude of −4 mm.

Factoring out the second and last term in Eq. 6, which are both $\propto \sin\frac{\psi}{2}$, one gets the sum $\left(\cos\alpha\sin\frac{\chi}{2} + (\vec{c}^{\,\rm bump}\cdot\vec{w})\sin\pi\nu_s\cos\frac{\chi}{2}\right)$. When the observed $p_0 = c_z$ values turned out to be at the level $-0.2... - 0.15$mrad at both solenoids, it means that the second term in the aforementioned sum is negligibly small. In order to increase sensitivity of the spin tune shifts to the second term in Eq. 6, the third flattop ΔT_3 should be used with opposite bump amplitude, while both solenoids would be running at the same settings in ΔT_2 and ΔT_3 .

1.5 Chromaticity correction

To set up the high precision spin tune measurement, a long spin coherence time of the order of a few hundred seconds is needed. Usually the sextupoles are set up such that vertical and horizontal chromaticities simultaneously vanish [7]. Fine tuning the sextupoles of the MXS and MXG families, one determines the location, where the spin coherence time (SCT) reaches the

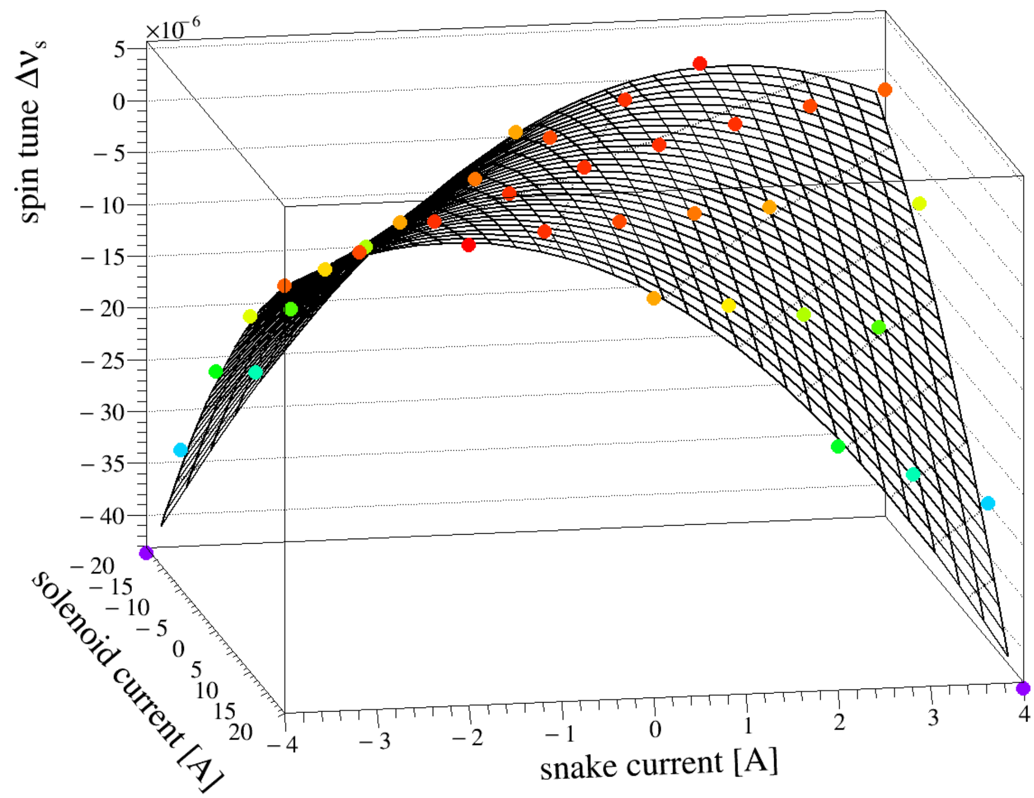

Figure 13: Spin tune map with the bump MSV 18-20-22 at the fixed amplitude of +3mm. The surface is a fit according to Eq. 7

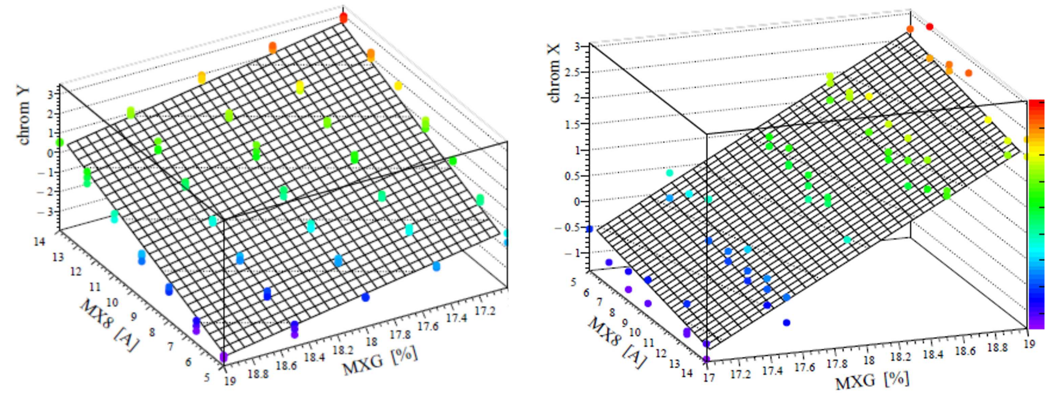

Figure 14: Example of the chromaticity scan with sextupoles of MXG family and one of MXL family sextupole MX8, near the compensation of both vertical and horizontal chromaticities.

optimum. Correction to zero chromaticity at MXG=12%, MXS=11.25 %, MXL=-1.5 %, brought SCT to $\approx$ 300s. Those sextupole settings were chosen as a “working point“- a fixed setting of sextupoles for all cycles, with optimal SCT. The reference orbit (see Fig. 7) during this measurement was used only for spin tune mapping with bumps, and the sextupoles were not optimized further to reach higher SCT, due to time constraints.

We also found out that not every setting for zero chromaticity correspond to long spin coherence time. Selection of the values for MXG and one of MXL (with name “MX8“) family sextupoles at which both vertical and horizontal chromaticities vanish (see Fig. 14), resulted at 60 seconds of SCT at best. The goal of such optimization was to achieve a working point for spin tune mapping with such bumps which pass through the unpowered MXS sextupole magnets. SCT scans with other sextupole families were also not promising (see Fig. 16). Perhaps, the culprit of the bad SCT was not optimal reference orbit, used for all SCT scans (Fig. 2).

However, there is an important indication of the robustness of the sextupole chromatic correction for high SCT. The measurement of 3 data points of spin tune map with the bump MSV 08-10-12 (see Fig. 15) were successfull. The bump was created passing through the working MXS-family sextupole MX5, which was set at $\approx$ 11%. For the bump amplitude of -7mm, vertical orbit shift in MX5 was -3.9 mm. When the amplitude of the bump was +5 mm, the orbit moved by +2.8 mm, at the location of MX5. The values for

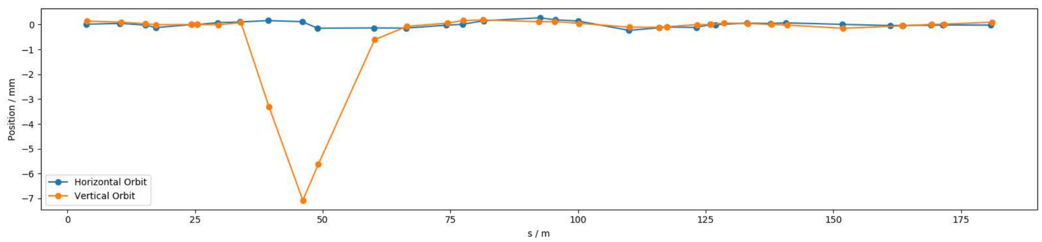

Figure 15: Example of the bump with steerers MSV 08-10-12. RMS orbit perturbation, excluding the BPMs within the bump, is: vertical 0.147 mm and horizontal 0.113 mm.

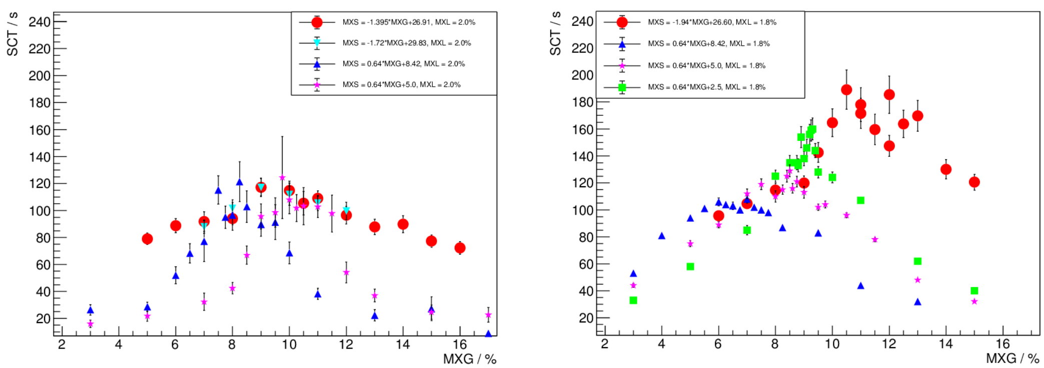

Figure 16: Spin coeherence time optimization with sextupoles of MXG and MXS family at fixed MXL family setting (left: MXL=2%, right: MXL=1.8%).

spin tune in ΔT_2 are in good agreement with the model and there was no decoherence of polarization observed. It means, vertical movement of the orbit in sextupole by almost 6mm does not affect the quality of the measurement method.

In the new experiment, we propose to use two working points from the SCT optimization, which are aimed to be used with two different sets of bumps among the 12 ones that we consider. They are both located on the so-called "final diagonal scan" (red circles on the right graph of Fig. 16) of SCT optimization. In the one set where bumps are crossing MXS family sextupoles, the working point is chosen with higher MXG and lower MXS values. For another set where bumps are crossing MXG family sextupoles, the MXG value should be lower, while MXS strength higher.

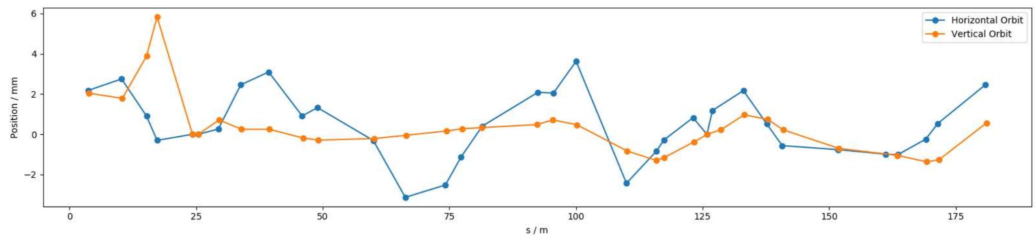

Figure 17: Difference of the reference orbits shown on Figs. 2 and 7.

2 Second stage: spin tune mapping with scaling of vertical orbit correction

Additive properties of $\vec{c}$ result from the linear dependance of the bump amplitude on the steerer settings. It is also true for the orbit as a whole, for linear dependance of orbit all over the ring from the power of vertical correctors. The difference of the reference orbits (Fig. 17) indicates that spin coeherence time is still at the order of 200 seconds even if significant change of the orbit occures. For example, by scaling all of the vertical steerer settings used for reference orbit at Fig. 7 by 50%, the change of $\Delta c_z = \Delta c_{sol} = 0.3$mrad can be observed at the location of 2MeV e-cooler solenoid. It allows to extrapolate Δc_z till the point of no orbit correction by steerers, thereby defining its contribution into measured values c_{sol} and c_{snake} (the fitted "p0" for spin tune maps at zero bump amplitude, SV20=0%, on Fig. 11).

3 Estimate of the required beam time

The measurements would require following timing:

- 200 seconds cycles are assumed, in which first 60 seconds is beam preparation
- a spin tune map with two bump amplitudes within a cycle is a mesh of solenoid currents, 7 by 7 points, with 2 cycles in each setting (which amount to 5.4 hours of continuous measurement)
- One spin tune map with three amplitudes of the bump: ≈16 hours
- 12 spin tune maps (one for each bump): 192 hours, or 8 days.

- SCT optimizations: 3-6 days depending on the need to choose the better working point with certain set of bumps
- total time for 1st stage: 11-14 days

Unpolarized cycles should not be used during the spin tune mapping, because determination of spin precession frequency, and therefore, the spin tune, does not depend on the initial polarization offsets. However, they are needed for the optimization of spin coherence time, when the in-plane polarization magnitude depends on the initial vertical polarization.

The second stage has lower priority than 1s stage, nevertheless it would require the same amount of time in total:

- same cycle structure assumed, where only 1 scaling of the vertical orbit in the cycle occurs to avoid beam losses (i.e. same as in Fig. 1, without 3rd time interval)
- same amount of points for spin tune map as in 1st stage: 2 cycles for the grid of 7 by 7 of solenoid currents, 200s per cycle
- 7 spin tune maps with predefined vertical orbit scales, including map at zero settings of all vertical steerers: $\approx$ 5 hours on each map
- $\approx$ 38 hours of continuos measurement for all maps (1.5 days)
- each spin tune map might require additional optimization of SCT, which takes up to 11 days in total
- repeat the measurements for all 7 maps to check for reproducability (1.5 days)
- 2nd stage: 14 days with polarized beam in total

The beam-based alignment of both solenoids should be performed with 7 predefined vertical orbit scales. Machine development time is distributed as follows:

- preparation of polarized deuteron beam at 970MeV/c, setting up electron cooling and polarimetry: 7 days
- beam-based alignment of solenoids, so that they do not perturb the orbit and work as spin rotators: 7 days

If the experiment conditions would not allow to complete the second stage, it should be repeated in another beamtime. It requires the same time block, as the two-staged experiment propesed here. In this case the time previously occupied by first stage is spent on such spin tune maps where global vertical orbit correction does not rely on the beam-based alignment of the solenoids.

Electron cooling is required after injection, acceleration, but before bunching the beam, to reduce polarization decoherence effects related to the momentum spread.

4 Roadmap to the future experiments to search EDM at storage rings

As a matter of fact, *we are creating local orbit distortion by horizontal magnetic fields in the ring and describing the resulting beam and spin dynamics.* Developed method is applicable in the future storage rings as a tool for diagnostics of beam and spin dynamics when approaching frozen spin condition. At prototype EDM ring, it can be applied at 30 MeV counter-circulating protons, to verify the achievements of the beam and spin-dynamic studies at pure magnetic rings with non-frozen spin. It is an important connecting step to test the model predictions for pure electrostatic lattice, preceding the measurements at strictly frozen spin condition.

5 Beam request

The JEDI collaboration would like to request beam time to collect data of seventeen spin tune maps. The experiment needs longer setup times related to strict requirements to set up the scaling of vertical orbit which is crucial for a smooth operation, and therefore **we request 2 weeks of machine development time and 4 weeks of measurement time**, to be scheduled at the earliest possible date.

References

[1] Lee, S. Y.: Spin Dynamics and Snakes in Synchrotrons (World Scientific, 1997) `https://www.worldscientific.com/doi/abs/10.1142/3233`

DOI 10.1142/3233

[2] Chao, A.: Handbook of Accelerator Physics and Engineering (World Scientific, 2013) `https://www.worldscientific.com/doi/abs/10.1142/8543` DOI 10.1142/8543

[3] Berz, M.: Computational aspects of optics design and simulation: COSY INFINITY. Nucl. Instrum. Meth. **A298**, 473–479 (1990). DOI 10.1016/0168-9002(90)90649-Q

[4] Eversmann, D., et al.: New method for a continuous determination of the spin tune in storage rings and implications for precision experiments. Phys. Rev. Lett. **115**, 094801 (2015). DOI 10.1103/PhysRevLett.115.094801

[5] Saleev, A., et al.: Spin tune mapping as a novel tool to probe the spin dynamics in storage rings. Phys. Rev. Accel. Beams **20**, 072801 (2017)

[6] Rathmann, F., Nikolaev, N.N., Slim, J.: Spin dynamics investigations for the EDM experiment at COSY `https://arxiv.org/pdf/1908.00350.pdf`.

[7] Guidoboni, G., et al.: Connection between zero chromaticity and long in-plane polarization lifetime in a magnetic storage ring. Phys. Rev. Accel. Beams **21**, 024201 (2018)